Cerebral Cortex May 2012;22:1038–1051
doi:10.1093/cercor/bhr172
Advance Access publication July 17, 2011

Failure to Modulate Attentional Control in Advanced Aging Linked to White Matter Pathology

Trey Hedden[1,2], Koene R. A. Van Dijk[1,3], Emily H. Shire[1,4], Reisa A. Sperling[1,4,5,6], Keith A. Johnson[2,5,6,7] and Randy L. Buckner[1,2,3,4,8]

[1]Athinoula A. Martinos Center for Biomedical Imaging, Department of Radiology, Massachusetts General Hospital, Charlestown, MA 02129, USA, [2]Department of Radiology, Massachusetts General Hospital, Harvard Medical School, Boston, MA 02115, USA, [3]Department of Psychology and Center for Brain Science, Harvard University, Cambridge, MA 02138, USA, [4]Department of Psychiatry, [5]Department of Neurology, Massachusetts General Hospital, Harvard Medical School, Boston, MA 02115, USA, [6]Center for Alzheimer Research and Treatment, Department of Neurology, Brigham and Women's Hospital, Boston, MA 02115, USA, [7]Division of Nuclear Medicine and Molecular Imaging, Massachusetts General Hospital, Harvard Medical School, Boston, MA 02115, USA and [8]Howard Hughes Medical Institute at Harvard University, Cambridge, MA 02138, USA

Address correspondence to Dr Trey Hedden, Athinoula A. Martinos Center for Biomedical Imaging, 149 13th Street, Suite 2301, Charlestown, MA 02129, USA. Email: hedden@nmr.mgh.harvard.edu.

Advanced aging is associated with reduced attentional control and less flexible information processing. Here, the origins of these cognitive effects were explored using a functional magnetic resonance imaging task that systematically varied demands to shift attention and inhibit irrelevant information across task blocks. Prefrontal and parietal regions previously implicated in attentional control were recruited by the task and most so for the most demanding task configurations. A subset of older individuals did not modulate activity in frontal and parietal regions in response to changing task requirements. Older adults who did not dynamically modulate activity underperformed their peers and scored more poorly on neuropsychological measures of executive function and speed of processing. Examining 2 markers of preclinical pathology in older adults revealed that white matter hyperintensities (WMHs), but not high amyloid burden, were associated with failure to modulate activity in response to changing task demands. In contrast, high amyloid burden was associated with alterations in default network activity. These results suggest failure to modulate frontal and parietal activity reflects a disruptive process in advanced aging associated with specific neuropathologic processes.

Keywords: aging, amyloid beta, executive function, fMRI, individual differences, PET

Introduction

Older adults often perform poorly in situations where multiple goals and response rules must be maintained and coordinated (Craik and Byrd 1982; Verhaeghen and Cerella 2002). These impairments may reflect a failure of attentional control (also referred to as executive function) with diverse effects on multiple domains including perception, memory, and language (Park et al. 2002; Gazzaley et al. 2005; Kemper et al. 2009). Here, we explored age differences in recruitment of brain systems associated with attentional control and their relationship to behavior and markers of neuropathology (West 1996; Buckner 2004; Hedden and Gabrieli 2004).

Attentional control is associated with a network involving prefrontal and parietal association regions commonly active during tasks that place high demands on controlled processing (Duncan and Owen 2000; Miller and Cohen 2001; Badre and Wagner 2004). Paradoxically, older adults often exhibit activity increases relative to younger controls within frontal and parietal regions when performing tasks, a response that has been interpreted as representing compensation (Reuter-Lorenz et al. 2000; Cabeza 2002; Cabeza et al. 2002; Grady 2002; Persson et al. 2004, 2006; Gutchess et al. 2005; Velanova et al. 2007; Holtzer et al. 2009; Rajah et al. 2010 although for opposing results, see Logan et al. 2002; Nielson et al. 2002; Langenecker and Nielson 2003; Colcombe et al. 2005; Duverne et al. 2009).

Recent models further suggest that age-related increases in activity occur with lower task demands where older adults maintain relatively intact performance but that age-related decreases in activity occur with higher task demands (Reuter-Lorenz and Cappell 2008; Lustig et al. 2009). By this view, increased activity may reflect "neural scaffolding" (Park and Reuter-Lorenz 2009) in response to age-related insults such as atrophy, white matter disruption, or amyloid deposition. At low levels of task demand, increased recruitment of available neural resources buttresses performance. Relative decreases emerge at high levels of task demand when available processing resources have reached their limit. To best probe age-associated differences, it is thus most informative to systematically vary difficulty and measure performance and the neural response at each level (Rypma et al. 2002; Mattay et al. 2006; Holtzer et al. 2009; Nagel et al. 2009; Schneider-Garces et al. 2009; Vallesi et al. 2011). An intriguing possibility is that an inability to modulate neural activity may itself be an important marker of disruption.

To explore this possibility, we collected data from an attentional control task that systematically varied task demands across separate blocks by requiring the inhibition of distracting stimuli, shifting between attentional foci, or both (Hedden and Gabrieli 2010). A large sample of clinically normal older adults was enrolled to allow detailed analysis of interindividual differences. We hypothesized that failure to modulate activity in frontal and parietal regions important to attentional control would relate to performance on executive function tasks and markers of neuropathology. Amyloid deposition and/or white matter abnormalities are present in a substantial proportion of clinically normal older adults. An open question is whether measures of white matter hyperintensities (WMHs), amyloid deposition, or both might affect attentional control.

Materials and Methods

Participants

Participants were 51 (49% females; aged 18–27 years, $M = 21.7$, standard deviation [SD] = 2.6) community-dwelling younger adults and 62 (58% females; aged 60–87 years, $M = 73.2$, SD = 6.4) community-dwelling

older adults. No participants exhibited evidence of mild cognitive impairment or dementia. Specifically, participants were excluded if they received a Clinical Dementia Rating (CDR) greater than 0, scored less than 27 on the Mini-Mental State Examination (Folstein et al. 1975), had been previously diagnosed with a neurological or psychiatric condition, had a history of head trauma, were taking more than 2 blood pressure or cholesterol medications, or presented with any safety contraindication for magnetic resonance imaging (MRI) or positron emission tomography (PET) imaging. All participants had normal or corrected to normal vision and were right handed. Participants provided informed consent in accordance with protocols approved by the Partners Healthcare Inc. Institutional Review Board. Because of time limitations and technical issues, estimations of WMHs were obtained for 54 of the 62 older adults, while PET amyloid imaging was performed on 49 of the 62 older adults. Portions of the clinical information and amyloid imaging data used to classify the participants' level of amyloid burden have been published previously (e.g., Buckner et al. 2009; Hedden et al. 2009). None of the functional MRI (fMRI) task data have been previously reported.

Demographic and Neuropsychological Measures

Participants were characterized on a number of commonly used demographic and neuropsychological instruments (Table 1). Socioeconomic status (SES) was measured with the Hollingshead SES scale, which separately ranks an individual's educational and occupational attainment on scales ranging from 1 to 7. A weighted score was computed by multiplying the educational score by 4 and the occupational score by 7 and summing the 2 scores (Hollingshead 1957). Lower scores indicate higher SES. Participants were asked to report the number of prescription medications they are currently taking and any chronic health conditions for which they have a current diagnosis. They were administered the American version of the National Adult Reading Test (Grober and Sliwinski 1991) to estimate full-scale IQ. Participants completed the Rey Auditory-Verbal Learning Test (RAVLT; Schmidt 1996) using a 30-min delayed interval (score indicates number of items recalled), pattern matching and number matching (Salthouse 1996) which are measures of speed of processing (for both, score indicates the number of items completed in 45 s), verbal fluency using the letters F, A, and S (FAS; score indicates the average number of items generated; Spreen and Benton 1977), the Letter-Number Sequencing subtest of working memory from the Wechsler Adult Intelligence Scale (WAIS-III) (score indicates the maximum number of items correctly held and reordered in memory; Wechsler 2002), and a sequence memory task in which participants had to report the order of 7 tests they had previously completed (participants were provided with visual cues and a brief description of each task; error score indicates the sum of the absolute difference between each item's correct placement and the participant's placement in the sequence). In a separate session, older adults (but not younger adults) were assessed with the CDR Scale (Morris 1993), the Geriatric Depression Scale (Yesavage et al. 1983), category fluency (animal and vegetable), the Digit-Symbol, Logical Memory, and Backward Digit Span subtests from the WAIS-III (Wechsler 2002), and Trail Making A and B (Reitan 1955).

For older adults only, composite measures of executive function, speed of processing, and episodic memory were constructed from the available neuropsychological variables as follows. First, *z*-scores were computed for each variable and variables for which lower scores indicated better performance were reverse scaled (by multiplying by −1). Second, confirmatory principle component analyses were conducted to construct separate composite constructs (components) for executive function, speed of processing, and episodic memory. For each analysis, 3 indicator variables were entered and only the first extracted component was used. Missing values (4.3% of the data) were replaced with the mean for that indicator variable. For executive function, the variables used (with unrotated component loadings in parentheses) were the *z*-score transformations of Letter-Number Sequencing (0.75), Backward Digit Span (0.72), and Trail Making B minus A (0.65). The component accounted for 50% of the variance among these 3 executive function variables. It is worth noting that the 2 highest-loading variables are both indicators of working memory, so this executive function composite could also be thought of as a working memory composite. For speed of processing, the variables used were the *z*-score transformations of Digit-Symbol (0.75), pattern matching (0.84), and number matching (0.85). The component accounted for 66% of the variance among the speed of processing variables. For episodic memory, the variables used were the *z*-score transformations of delayed recall from Logical Memory (0.53), sequence memory (0.73), and 30-min delayed recall from the RAVLT (0.84). The component accounted for 51% of the variance among the episodic memory variables. Factor scores representing each composite were computed for each individual participant.

Table 1
Demographic and neuropsychological characteristics of participants

Dependent measure	Younger		Older			
			Modulating		Nonmodulating	
	M	SD	*M*	SD	*M*	SD
N	51		38		24	
Age	21.7	2.6	72.7	6.7	74.3	5.8
MMSE	29.1	0.9	29.3	0.8	29.1	1.1
CDR sum of boxes	—	—	0.1	0.3	0.1	0.3
Geriatric Depression Scale	—	—	4.6	3.8	4.2	4.3
Education (years)[a]	14.9	1.6	16.0	2.4	17.2	2.7
Hollingshead SES[b]	23.2	7.0	28.5	8.2	23.3	9.4
# Medications[a]	0.5	0.6	2.7	2.3	2.8	1.8
# Health conditions[a]	0.0	0.3	0.7	0.9	0.8	1.0
FAS	15.5	3.8	15.9	4.5	16.6	3.8
AMNART estimated IQ	117.7	4.7	121.1	7.4	119.3	8.2
Letter-Number Sequencing[a]	14.7	2.8	11.1	2.3	10.2	1.7
Backward Digit Span	—	—	8.4	1.9	7.4	2.3
Trail Making B–A	—	—	37.6	14.9	50.4	34.5
Pattern matching[a]	20.9	2.8	12.7	2.8	11.4	2.2
Number matching[a]	29.5	0.9	25.2	3.5	23.9	3.1
Digit-Symbol	—	—	53.8	11.0	50.0	9.6
RAVLT (30 min recall)[a]	13.1	2.1	10.0	4.2	9.3	3.4
Sequence memory[a]	4.6	3.7	7.8	3.9	8.2	4.5
Logical Memory	—	—	14.3	3.9	15.0	3.6
Executive function composite[b]	—	—	0.24	0.85	−0.38	1.11
Speed of processing composite	—	—	0.20	1.04	−0.31	0.87
Episodic memory composite	—	—	0.03	1.00	−0.05	1.02

Note: MMSE, Mini-Mental State Examination; AMNART, American version of the National Adult Reading Test; RAVLT, Ray auditory-verbal learning test; FDR, false discovery rate.
[a]Main effect of age, $P < 0.05$, FDR corrected.
[b]Significant difference between older modulating and nonmodulating groups, $P < 0.05$, FDR corrected. Higher Hollingshead SES scores indicate lower estimated SES. Some neuropsychological measures were administered in a separate session completed by the older adults only; data is therefore not available for the younger adults. Composite scores are in *z*-score units representing SD units away from the older group mean ($M = 0$).

MRI Data Acquisition

Participants underwent fMRI on a Siemens TrioTIM 3.0-T scanner (Siemens, Erlangen, Germany) equipped with a 12-channel phased-array whole-head coil. Visual stimuli were generated using an Apple PowerBook G4 (Apple, Inc., Cupertino, CA) running Psychtoolbox (Brainard 1997; Pelli 1997) within Matlab (The Mathworks, Inc., Natick, MA) and projected onto a screen positioned at the head of the magnet bore and reflected onto a mirror affixed to the head coil. Head motion was restrained with a foam pillow and extendable padded head clamps. Earplugs were used to attenuate scanner noise. All participants wore MR-compatible glasses and lenses (participants not needing corrective lenses wore 0.0 diopter lenses). High-resolution 3D T_1-weighted magnetization prepared rapid acquisition gradient echo (MP-RAGE) anatomical images were collected with the following parameters: time repetition (TR) = 2300 ms, time echo (TE) = 2.98 ms, flip angle (FA) = 9°, 1 × 1 × 1.2 mm voxels. Functional data were acquired using a gradient-echo echo-planar pulse sequence sensitive to blood oxygenation level–dependent (BOLD) contrast (Kwong et al. 1992; Ogawa et al. 1992) using the following parameters: TR = 2500 ms, TE = 30 ms, FA = 88°, 3.03 × 3.03 ×3 mm voxels. Thirty-nine transverse slices aligned to the AC–PC plane covered the whole brain. Functional images were acquired during

performance of the attention task in 3 runs of 108 time points. Fluid attenuation inversion recovery (FLAIR) images for visualization of white matter lesions were collected with the following parameters: TR = 6000 ms, TE = 455 ms, TI = 2100 ms, 1 × 1 × 1 mm voxels.

Task Description

The global–local behavioral task used to measure attentional control consisted of hierarchical letter stimuli of the type described by Navon (1977) using methods similar to those implemented in a prior imaging study (Hedden and Gabrieli 2010). Stimuli consisted of large letters (H, S, and O) made up of small letters (H, S, and O) (Fig. 1). Small letters subtended a visual angle of approximately 0.8° × 0.6°; large letters subtended approximately 4.8° × 3.3°. Stimuli were presented in either green or blue on a black background. Participants were pretested both outside and inside the scanner to ensure that they could clearly see the stimuli, discern the colors, and perform the task as instructed. Participants were instructed to identify either the global (large letter) or the local (small letter) level on each trial, as cued by the color, and to respond with the appropriate response (either H or S). The letter O was never mapped to a response and was therefore used for neutral conditions. Neutral stimuli contained an O at the unattended level and an H or S at the attended level. Incongruent stimuli contained incompatible letters (H and S) at opposing levels. Congruent stimuli containing the same letter (either H or S) in both the global and the local levels were not used because results from a prior study (Hedden and Gabrieli 2010) found that inhibitory effects could be estimated from the contrast of incongruent versus neutral. Stimuli were organized into blocks of 10 trials, which could either involve shifting of attention or not. In nonshift blocks, participants were cued to constantly attend to either the global or the local level. In shift blocks, participants were cued by the stimulus color (blue or green) to predictably shift between attending to the global and local levels. Combining the neutral and incongruent stimuli with the nonshift and shift blocks resulted in 4 possible block types: neutral nonshift (NN), neutral shift (NS), incongruent nonshift (IN), and incongruent shift (IS). Two blocks of each condition were presented during each imaging run, for a total of 6 blocks per condition (60 trials per condition). On each trial, the stimulus was presented for 2000 ms, followed by an intertrial interval of 500 ms during which a fixation crosshair was displayed. Right-handed key press responses were collected using an MRI-compatible button box. A fixation crosshair was presented for a constant period of 20 s at the beginning, middle, and end of each imaging run to allow estimation of a rest baseline. Participants received extensive instruction, with 48 self-paced practice trials and 84 timed practice trials before entering the scanner, and an additional 48 timed practice trials immediately prior to the start of the task once inside the scanner.

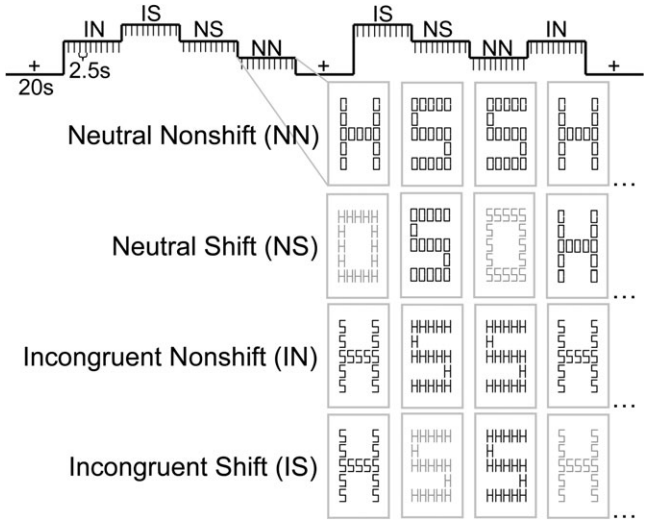

Figure 1. Schematic representation of the global–local task. Participants viewed hierarchical letter stimuli (e.g., a large S made of small Hs) and responded by identifying either the global (large) or local (small) letter, as cued by the color of the stimulus. Participants completed blocks of 10 trials each from 1 of 4 conditions. Neutral blocks involved stimuli in which one level (global or local) was not mapped to a response (the letter O); incongruent blocks involved stimuli in which the 2 levels had conflicting letter stimuli. In nonshift blocks, participants responded to the same stimulus level for all 10 trials (i.e., the color of the stimuli did not change across trials); in shift blocks, participants were cued by the stimulus color to predictably shift between the global and local levels. Fixation blocks 20 s in duration occurred at the beginning, middle, and end of each run. Participants completed 3 task runs of pseudorandom block order. Color cues used were blue and green (here depicted as black and gray); stimuli were presented on a black background.

fMRI Data Analysis

The first 4 volumes of each run were discarded to allow for T_1-equilibration effects and the acquired runs were concatenated, with effects of run modeled in the general linear model (GLM). Slice acquisition dependent time shifts were corrected per volume (SPM2, Wellcome Department of Cognitive Neurology, London, UK). Then, rigid body translation and rotation were used to correct for head motion (Jenkinson et al. 2002; FMRIB, Oxford, UK) and atlas registration was achieved by computing affine transforms connecting the first volume of the functional run (Jenkinson and Smith 2001; FMRIB, Oxford, UK), with a T_2 EPI template based on a merged data set of younger and older adult brains (Buckner et al. 2004) that has been mapped to the Montreal Neurological Institute (MNI) atlas space (Evans et al. 1993). Motion correction and atlas transformation parameters were applied in a single step in which all data were resampled to 2-mm isotropic voxels. Data were spatially smoothed using a 6-mm full-width at half-maximum Gaussian kernel. The GLM was conducted in SPM2 and modeled each condition as a boxcar regressor convolved with a hemodynamic response function including temporal derivatives and included regressors for run effects and linear drift. Group-level analyses were conducted by selecting contrasts of interest for each participant and entering them in second-level random-effects *t*-tests (see Fig. 2). Surface mapping of the group-level results was conducted using CARET 5.612 (Van Essen et al. 2001). These exploratory analyses were primarily used to validate the independent, a priori selection of regions of interest (ROIs; see below) and to visualize the full regional topography of activity in each group.

Hypothesis-Driven Analyses

ROIs associated with attentional control were defined on an a priori basis using a previous data set of 17 younger adults (Hedden and Gabrieli 2010). Data from this previous study were used to identify prefrontal and parietal cortical regions from the incongruent shift versus neutral nonshift (IS > NN) contrast that also displayed significantly greater activity in the neutral shift condition than in the neutral nonshift condition (NS > NN) and significantly greater activity in the incongruent nonshift condition than in the neutral nonshift condition (IN > NN). Thirteen prefrontal and parietal ROIs were identified and carried forward for analysis in the current data set. One additional region, with MNI coordinates $x = -34$, $y = 22$, $z = 4$, that did not meet these criteria was also included because it is the left homologue of a region identified in right inferior frontal gyrus with coordinates $x = 34$, $y = 26$, $z = 2$. These 14 ROIs were defined using 6-mm radius spheres around the peak coordinates in MNI template space (for ROI placement, see Supplementary Fig. *A* and for peak coordinates, anatomical location, and Brodmann area label for each ROI, see Supplementary Fig. *C*). The average relationship among activity values across all conditions within these 14 regions was estimated using Cronbach's alpha and was 0.97 for younger adults and 0.97 for older adults, suggesting that it was reasonable to combine ROIs into an aggregate measure. Activity values (beta values from each participant's GLM) were extracted from each ROI for each condition and the mean activity value across all ROIs was computed for each participant.

For each participant, the slope of the mean activity across conditions was calculated by fitting a regression line to the mean beta value from each condition (assuming an equivalent interval between all conditions, for discussion of this assumption, see Supplementary Methods). This slope of activity was treated as a continuous measure and used as the

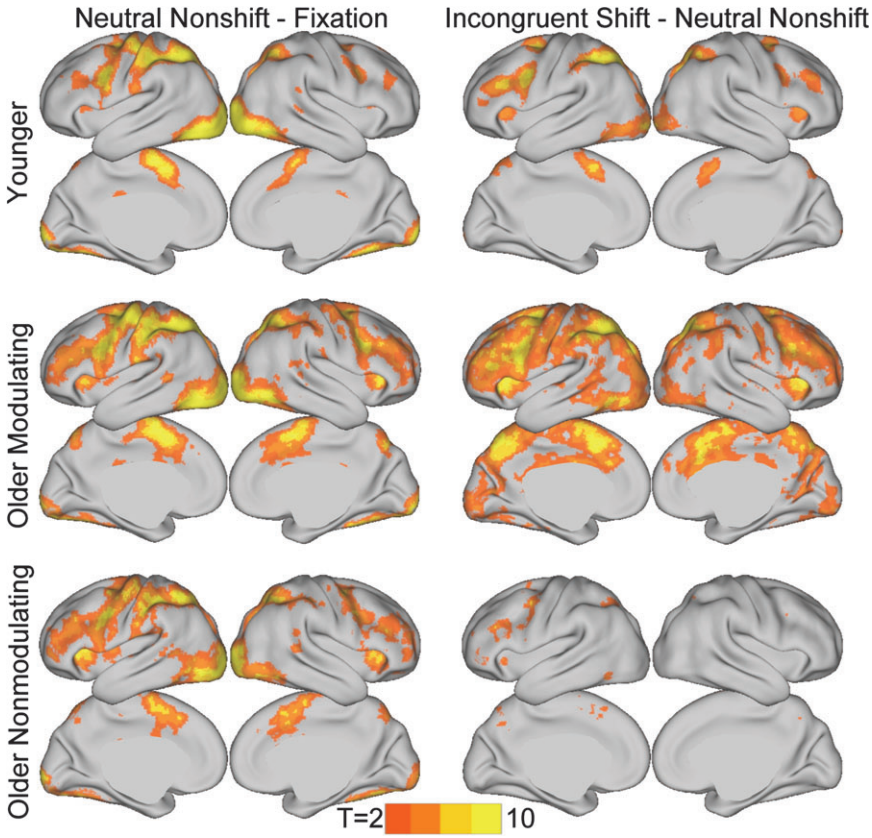

Figure 2. Activity maps for younger, older modulating, and older nonmodulating groups. Group-level maps of the BOLD response (an indirect measure of neuronal activity) were computed for each group using second-level random-effects analysis and are displayed at a threshold of $t > 2$ for visualization purposes only. Both modulating and nonmodulating older adults exhibited increased activity in prefrontal and parietal cortex relative to younger adults in the contrast of Neutral Nonshift–Fixation, whereas only the modulating older adults exhibited such increased activity in the contrast of Incongruent Shift–Neutral Nonshift. Because the groups were defined based on activity patterns it is unsurprising that nonmodulating older adults showed very little activity differences in the latter contrast. Note that the ROIs used in the hypothesis-driven analyses were defined from an independent data set without respect to these activity maps, which are shown only to provide a qualitative view of the regional topography.

primary dependent measure in regression analyses. In order to better visualize certain key effects from these main analyses, a supplementary subgroup classification was conducted on the older participants. Older participants who exhibited a monotonic or asymptotic increase across conditions (NN, NS, IN, IS) were classified as "modulating," indicating that their mean neural response in the defined ROIs was affected in the expected direction by the changing task conditions. Participants who exhibited a relatively flat or nonincreasing pattern across conditions were classified as "nonmodulating," indicating that their mean neural response in the defined ROIs was not sensitive to the changing task conditions. Specifically, this classification was done using the following algorithm. The mean, SD, and 95% confidence intervals of the slope of activity were computed across all participants. Because there were no significant differences between the distributions of the slope of activity measurement between younger and older adults (see Results), all participants were included as the reference group. Participants with an individual slope value greater than the group's lower bound of the 95% confidence interval (slope ≥ 0.098) were classified as modulating, while participants with a slope value less than the lower bound of the 95% confidence interval (i.e., not significantly different from 0) were classified as nonmodulating. Note that if only older adults are used as the reference group, the lower bound of the 95% confidence interval is not significantly different (slope ≥ 0.094) and applying this value does not significantly alter any reported results.

An additional set of 6 ROIs were selected to target the default network (Shulman et al. 1997; Raichle et al. 2001; Buckner et al. 2008). These regions were taken from a previous study using functional connectivity analyses and were defined from an independent sample of 48 younger adults (described in Hedden et al. 2009; Van Dijk et al. 2010). These 6 regions were used as ROIs by defining 6-mm radius spheres around the peak coordinates in MNI template space (for ROI placement, see Supplementary Fig. *A*). The coordinates used were $x = 0$, $y = -53$, $z = 26$ in the posterior cingulate cortex, $x = 0$, $y = 52$, $z = -6$ in the medial prefrontal cortex, $x = -48$, $y = -62$, $z = 36$ and $x = 46$, $y = -62$, $z = 32$ in the left and right lateral inferior parietal cortex, and $x = -24$, $y = -22$, $z = -20$ and $x = 24$, $y = -20$, $z = -22$ in the hippocampal formation. The average relationship among activity values across all conditions within these 6 regions was estimated using Cronbach's alpha and was 0.95 for younger adults and 0.86 for older adults, suggesting that it was reasonable to combine ROIs into an aggregate measure. Activity values (beta values from each participant's GLM) were extracted from each ROI for each condition and the mean activity value across all ROIs was computed for each participant.

Amyloid Imaging Acquisition

Amyloid burden was measured with *N*-methyl-[^{11}C]-2-(4-methylaminophenyl)-6-hydroxybenzothiazole (Pittsburgh Compound B; PiB), which binds to fibrillar amyloid and was prepared at Massachusetts General Hospital as described previously (Klunk et al. 2001, 2004; Mathis et al. 2002). Participants underwent PiB PET imaging as described previously (Gomperts et al. 2008; Hedden et al. 2009; Sperling et al. 2009). Briefly, data were acquired using a Siemens/CTI ECAT HR+ scanner (3D mode; 63 image planes; 15.2-cm axial field of view; 5.6-mm transaxial resolution and 2.4-mm slice interval; 69 frames: 12 × 15 s, 57 × 60 s). After a transmission scan, 8.5–15 mCi [^{11}C]-PiB was injected as a bolus and followed immediately by a 60-min dynamic acquisition. PET data were reconstructed and attenuation corrected, and each frame was evaluated to verify adequate count statistics and absence of head motion.

Amyloid Imaging Analysis

The dynamic PET images were reconstructed with scatter correction using commercially available routines for 3D PET data. PET images (0–8 min of initial uptake) were registered and normalized to an MRI MNI template using SPM2. The distribution volume ratio (DVR) was employed based on the Logan graphical analysis technique (Logan et al. 1990) that has been fully validated for PiB imaging (Price et al. 2005). Time-activity curves were measured in each brain region under analysis (ROI or voxel) and in a reference region in cerebellar cortex known to contain low levels of fibrillar amyloid. This approach has been applied to numerous PiB studies (e.g., Lopresti et al. 2005; Price et al. 2005; Fagan et al. 2006; Johnson et al. 2007) and yields data that are similar to arterial blood input methods (Lopresti et al. 2005).

Each individual's mean image was examined and an index of PiB presence in cortical regions was calculated using the dynamic data via Logan graphical modeling within a large aggregate cortical ROI consisting of frontal, lateral parietal and temporal, and retrosplenial cortices (the FLR region). PiB retention in the FLR region is substantial in patients with diagnosed Alzheimer's disease (AD) and has been used as a summary measure of PiB retention in previous studies (Johnson et al. 2007; Gomperts et al. 2008; Hedden et al. 2009). In the current sample of 49 clinically normal older adults who underwent amyloid imaging, PiB DVR values in the FLR region were highly correlated with global PiB retention ($r = 0.99$) and with ROIs located in the precuneus ($r = 0.89$), posterior cingulate ($r = 0.90$), and frontal cortices ($r = 0.98$), supporting the use of FLR as an aggregate measure.

In an effort to ensure that partial-volume effects did not account for the results and to examine the impact of more specific regional PiB deposition, we regressed average cortical thickness within each cortical region derived from a FreeSurfer parcellation of coregistered MRI data (see Supplementary Methods) on PiB DVR (Becker et al. 2010). We then examined the average partial-volume corrected DVR values from each FreeSurfer ROI for relationships to the dependent variables of interest. Regions selected from the frontal cortex were the frontal pole, superior frontal, rostral and caudal middle frontal, pars opercularis, pars triangularis, pars orbitalis, lateral and medial orbitofrontal, and rostral and caudal anterior cingulate; from the parietal cortex regions selected were superior parietal, inferior parietal, supramarginal, precuneus, posterior cingulate, and the isthmus of the cingulate (Desikan et al. 2006). The average correlation of these region-specific partial-volume corrected DVR values with the uncorrected FLR DVR used in the main analyses was $r = 0.73$, $P < 0.001$ (ranging from $r = 0.55$ in the pars orbitalis to $r = 0.85$ in the pars triangularis). As the results reveal, the conclusions are unchanged when region-specific partial-volume corrected DVR values are used.

On the basis of observed PiB DVR values in the FLR region, participants were classified into 2 groups: 21 PiB positive (PiB+) individuals, who displayed extensive increased PiB retention (defined as greater than FLR DVR ≥ 1.15) and 28 PiB negative (PiB–) individuals, who displayed insubstantial PiB retention (FLR DVR < 1.15). This PiB cutoff value was selected a priori to be comparable to previous reports (Johnson et al. 2007; Gomperts et al. 2008; Hedden et al. 2009) and to ensure that individuals classified as PiB– were well outside the range of PiB values observed in AD patients (Hedden et al. 2009). PiB retention (defined as FLR DVR) was treated as a continuous variable to ensure that the selection of a cutoff value did not dictate the results. Additionally, the classification of PiB– and PiB+ was also used as a variable of interest to examine the potential for effects of amyloid only in those with elevated retention. Individuals classified as PiB+ were not significantly older ($M = 73.9$, SD = 7.5, 61–87) than those classified as PiB– ($M = 72.3$, SD = 6.1, 60–84) and there was not a significant correlation between age and PiB retention ($r = 0.22$, $P = 0.13$); nonetheless, all reported results involving PiB controlled for age.

WMH Analyses

WMHs were identified from each individual's FLAIR image for 54 of the older adults using an automated fuzzy-connected algorithm (see Supplementary Fig. *B*) that has been previously validated against a visual grading system (Wu et al. 2006). This automated WMH segmentation method involves 1) automatic identification of WMH seeds based on the intensity histogram of the FLAIR image, 2) using a fuzzy-connected algorithm to segment the WMH clusters, 3) iteratively updating the set of seeds, and 4) combining the WMH clusters into a final WMH segmentation. The histogram of the skullstripped (BET; Smith 2002) FLAIR image was used to define a threshold, which was set to be the mean ± 2.5 SDs. This method of WMH segmentation enables different thresholds for seed growing at each WMH cluster and avoids a single cutoff threshold for the whole volume. From the resulting WMH segmentation, we extracted the total WMH volume in mm^3 within a mask defined by the Johns Hopkins University White Matter Atlas (Wakana et al. 2004), which was reverse normalized to the native space of each individual's FLAIR image. Because the automated algorithm is designed to detect regions of relative hyperintensity, this can lead to false detections, particularly in individuals with little or no areas of true hyperintensity (as in younger adults). Assumptions built into the algorithm, such as the threshold applied and the regions included in the mask, may introduce systematic bias; however, the classification and ordering of individuals by the resulting WMH estimates appear to be robust to changes in these assumptions. Because of the potential for bias, the resulting WMH images were manually checked to ensure that false detections did not substantially contribute to a participant's WMH volume estimate.

Younger adults had virtually no detectable regions of WMH, while the older adults had substantial WMH volumes ($M = 2442$, SD = 3384). Within the older adult group, it was clear that a large proportion of the sample had relatively small WMH volumes, although still detectable, while a subset of the sample had substantially elevated WMH volumes. In keeping with prior findings that a threshold level of WMH may be required before influences of this pathology are observed (e.g., Boone et al. 1992), we used an iterative outlier elimination process (e.g., Aizenstein et al. 2008) to identify that portion of the sample exhibiting relatively low WMH volumes (participants with WMH volumes < 2500 mm^3 were selected through this process, which required 3 iterations, and displayed volumes of $M = 742$, SD = 484). We then applied a threshold of 3 times the SD above the mean of this subset as our criterion for high WMH volumes, resulting in a threshold of 2194 mm^3, with 16 older individuals above this threshold (including all of those identified through the iterative elimination process) and 38 below this threshold. This threshold corresponded to a natural break point in the data, as no participants exhibited WMH volumes between 1763 and 2306 mm^3. Participants above this threshold were classified as high in WMH volume (WMH+), while those below the threshold were classified as low in WMH volume (WMH–). Subsequent analyses revealed that results are not meaningfully dependent upon this choice of threshold, although applying a more conservative (i.e., higher) threshold value tends to result in stronger effects for the results described, whereas applying a more liberal (i.e., lower) threshold value tends to result in weaker effects (effects are still qualitatively apparent at thresholds down to 922 mm^3). Although we report raw WMH volumes for transparency, we also examined the WMH as a percentage of estimated intracranial volume (computed from FreeSurfer parcellation, see Supplementary Methods) and as log-transformed values because of the nonnormal distribution of WMH values. Neither of these transformations had any significant impact on the reported results. WMH volume was treated as a continuous variable to ensure that the selection of a cutoff value did not dictate the results. Additionally, the classification of WMH– and WMH+ was used as a variable of interest to examine the potential for effects of WMHs only in those with elevated burden. Individuals classified as WMH+ were older ($M = 76.1$, SD = 5.5, 69–87) than those classified as WMH– ($M = 71.5$, SD = 6.5, 60–83) and there was a significant correlation between age and WMH volume ($r = 0.35$, $P = 0.01$); for this reason, all reported results involving WMH controlled for age. There was also an association between WMH volume and a summary measure of vascular risk ($r = 0.31$, $P < 0.05$), however, this correlation was not significant when controlling for age ($r = 0.20$, $P = 0.15$); additional details are reported in the Supplementary Materials.

Results

Older Adults Exhibit Increased Activity in a Widespread Set of Regions Related to Attentional Control

Based on the results of a previous study (Hedden and Gabrieli 2010), a priori ROIs in frontal and parietal cortices were examined for age-related differences (Supplementary Fig. *A*).

Although independently identified, these ROIs corresponded closely to the topography of activity in the current data set where increases in activity in prefrontal and parietal cortices were clearly visible among the older adults compared with younger adults, as can be seen in Figure 2. Activity (beta values from the GLM) relative to baseline (fixation) was computed for each condition (neutral nonshift, neutral shift, incongruent nonshift, and incongruent shift) in the global–local task for each ROI and subjected to an Age Group (2) × Condition (4) analysis of variance (ANOVA). In each ROI, older adults exhibited significantly greater activity than did younger adults (see Supplementary Fig. *C*). Activity between regions was highly related (Cronbach's alpha = 0.97), allowing the computation of an aggregate ROI response (mean of all ROIs). This aggregate ROI also exhibited a main effect of age group, with greater activity in older than in younger adults, $F_{1,111} = 48.08$, $P < 0.001$ (see Fig. 3). In the aggregate ROI, both younger and older adults exhibited an increase in activity as the difficulty of the task condition increased, $F_{3,109} = 61.29$, $P < 0.001$, although there was no interaction of age group and task condition. These results confirm the predominant finding in the literature that older adults exhibit increased activity in task-related regions, especially those in the prefrontal and parietal cortices, during the performance of attentionally demanding tasks (e.g., Grady et al. 1998; Reuter-Lorenz et al. 2000; Cabeza et al. 2002; Logan et al. 2002; Velanova et al. 2007; for a recent review, see Spreng et al. 2010).

A Subset of Older Individuals Fail to Modulate Activity in Response to Task Demands

We structured the global–local task conditions to require participants to dynamically allocate attention as task demands changed across conditions. We hypothesized that such dynamic allocation of attention would be associated with increasing levels of activity as task demands increased and that failures of dynamic allocation of attention could be observed in some individuals through a lack of modulation of activity in response to changing task conditions. To examine this issue, we computed individual estimates of the slope of activity in the aggregate ROI across task conditions. Older individuals were classified into groups with modulating and nonmodulating activity profiles on the basis of this slope (see Materials and Methods). A modulating activity profile indicates a clear increase in activity across task conditions, whereas a nonmodulating profile indicates little to no increase across conditions. Note that the slope of activity indicates only the extent of the linear pattern of the increase across conditions and does not represent the overall magnitude of activity (detailed above). Twenty-four of the older adults (38.7%) were classified as having nonmodulating activity profiles. The group differences in activity profiles for the aggregate ROI are depicted in Figure 3. Notably, in both younger and older groups, the slope measurement exhibited a normal distribution (Supplementary Fig. *D*); for this reason, our primary analyses treat slope as a continuous measure. There were no age differences in the slope measurement itself (younger: $M = 0.11$, SD = 0.08, older: $M = 0.12$, SD = 0.10) and both age groups displayed equivalent distributions on this measurement (Kolmogorov–Smirnov $z = 0.70$, $P = 0.71$). Of critical interest to our hypotheses was whether lower slopes of activity among older adults would be associated with poorer performance and with increased white matter or amyloid neuropathology.

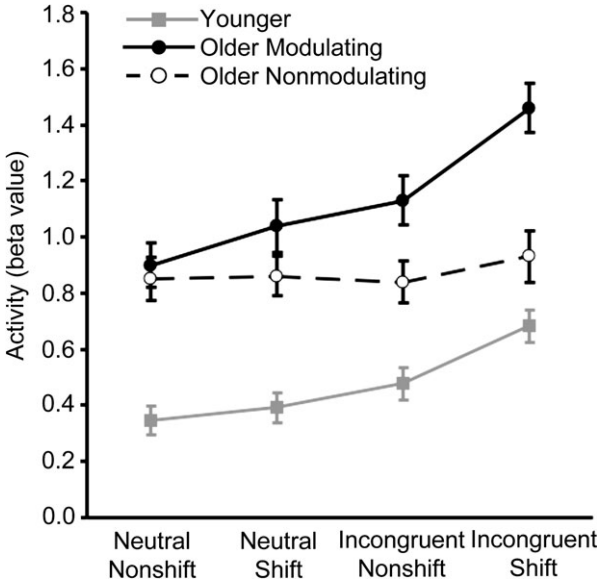

Figure 3. Activity in each condition for younger adults and for modulating and nonmodulating older adults averaged across all ROIs. Modulating individuals show an increase in activity across task conditions, whereas nonmodulating individuals show no increase in activity across conditions. Older adults (both modulating and nonmodulating) exhibited increased magnitude of activity relative to younger adults.

Older Adults Failing to Modulate Activity Perform Poorly as Task Demands Increase

We hypothesized that older individuals with nonmodulating activity profiles were failing to dynamically allocate attention and would therefore demonstrate poorer performance in the more demanding conditions than individuals with modulating profiles. To test this hypothesis, we entered accuracy from each condition into a Group (3) × Condition (4) ANOVA. Supporting our hypothesis, there was a Group × Condition interaction, $F_{6,218} = 8.52$, $P < 0.001$, such that older adults with nonmodulating activity profiles exhibited poorer accuracy as task demands increased than did older adults with modulating profiles, and both older groups were less accurate than younger adults as task demands increased (Fig. 4). A planned comparison indicated a significant interaction of Group × Condition when comparing only the older groups, $F_{3,180} = 4.66$, $P < 0.01$. There was no significant difference between modulating and nonmodulating older adults in the least demanding condition (NN: $t_{60} = 1.84$, $P = 0.07$), but this difference was significant in all other conditions (smallest $t_{60} = 2.82$, $P < 0.01$). Because the slope measure used to classify older individuals into groups with modulating and nonmodulating profiles displayed a normal distribution (rather than a bimodal distribution showing 2 clear groups), we examined the correlation between the slope of activity across conditions and performance in each condition. Among older adults, a significant correlation between slope of activity and accuracy was not observed in the least demanding condition (NN: $r = 0.21$, $P = 0.10$) but was observed in all conditions in which some degree of attentional allocation was required (NS: $r = 0.37$, $P = 0.003$; IN: $r = 0.40$, $P = 0.001$; IS: $r = 0.27$, $P = 0.04$). The observed relationships suggest that older adults who fail to modulate activity across conditions are those most susceptible to performance decrements in individual conditions. In contrast, for younger adults, there

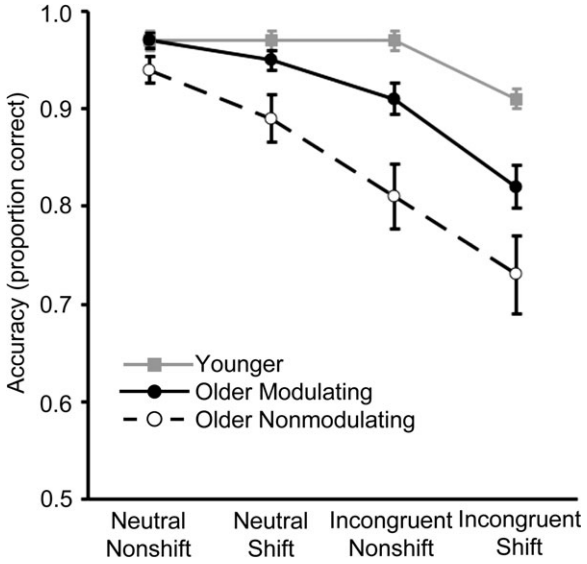

Figure 4. Accuracy in each condition for younger adults and for modulating and nonmodulating older adults. Modulating older individuals showed better relative performance across task conditions, whereas nonmodulating older individuals showed a steeper decrease in performance across conditions. Both modulating and nonmodulating older adults showed decreased performance across task conditions relative to younger adults.

was no significant correlation between slope of activity and accuracy in any individual condition (NN: $r = 0.15$, $P = 0.30$; NS: $r = 0.10$, $P = 0.51$; IN: $r = -0.08$, $P = 0.56$; IS: $r = -0.19$, $P = 0.19$). For additional analyses regarding the relationship of the slope of activity and performance, see the Supplementary Materials and the analyses exploring the potential influences of WMH and amyloid pathology detailed below.

Failure to Modulate Activity Is Related to Poorer Executive Performance on Independent Neuropsychological Tasks

We examined the relationship between modulation of activity during the global–local task and performance on an independent neuropsychological battery that measured executive function, speed of processing, and episodic memory. Composite measures of each neuropsychological construct were computed (see Materials and Methods) and differences between modulating and nonmodulating older adults were examined in planned *t*-tests (*M* and SD displayed in Table 1). Older adults with a modulating activity profile performed significantly better than those with a nonmodulating profile on the executive function composite, $t_{60} = 2.51$, $P = 0.02$ and the speed of processing composite, $t_{60} = 1.99$, $P = 0.05$ but not on the memory composite, $t_{60} = 0.30$, $P = 0.77$. The mean difference between modulating and nonmodulating older adults on the executive function composite represents approximately a 0.6 SD advantage in performance for individuals with a modulating activity profile. However, these results were not significant when treating slope of activity as a continuous measure (executive function: $P = 0.13$, speed: $P = 0.25$, episodic memory: $P = 0.78$). Controlling for age, WMH volume (largest relationship with executive function, $P = 0.25$) and PiB retention (largest relationship with memory, $P = 0.17$) were not significantly related to these composite measures. When entered as controlling variables, neither WMH volume nor PiB retention significantly accounted for the effects of modulation of activity on the composite neuropsychological measures.

Modulation of Activity, Rather than Magnitude of Activity, Explains Decreases in Performance

An alternative hypothesis is that the generally higher absolute magnitudes of activity exhibited by older adults may be indicative of compensatory recruitment of attentional control. It is apparent from Figures 2 and 3 that older adults with modulating and nonmodulating activity profiles have equivalent magnitudes of activity in the least demanding task condition (neutral nonshift) but that older adults with modulating profiles exhibit increased activity with greater task demands. Therefore, older adults with modulating profiles ($M = 1.13$, SD = 0.51) will also exhibit a higher average magnitude of activity across task conditions than older individuals with nonmodulating profiles ($M = 0.87$, SD = 0.36), $t_{60} = 2.17$, $P = 0.03$. To assess whether the average magnitude of activity fully accounted for the relationship between the slope of activity and task performance, we included the average magnitude of activity in all subsequent regression models. Significant effects of slope of activity therefore indicate effects above and beyond those accounted for by the magnitude of activity. The mean magnitude of BOLD-measured activity did not account for the effects attributable to the slope of accuracy. As an additional test of this alternative hypothesis, we used a median split to divide the older participants into those with relatively greater and lesser average magnitudes of activity. These 2 groups did not differ on any measure of accuracy nor on any of the independent neuropsychological composites.

Amyloid and WMHs Represent Distinct Neural Pathologies

WMH volume was not correlated with amyloid burden (entering both measures as continuous variables), $r = 0.02$, $P = 0.88$. If WMH volume and amyloid burden are log transformed to account for skewness in the distributions, the correlation remains nonsignificant, $r = 0.05$, $P = 0.73$. These results are not altered when age is partialled. Very few individuals displayed both elevated amyloid burden and elevated WMH volumes (Fig. 5). A chi-square test indicated that fewer individuals than would be expected by chance had both elevated amyloid burden and elevated WMH burden ($\chi^2 = 8.55$, $P < 0.05$).

WMH Volume, But Not Amyloid Burden, Is Associated with Failures to Modulate Activity

Based on previously found associations between changes in white matter and cognition including executive function (Boone et al. 1992; DeCarli et al. 1995; De Groot et al. 2000, 2002; Gunning-Dixon and Raz 2000; O'Sullivan et al. 2001; Kennedy and Raz 2009; Zahr et al. 2009), we hypothesized that older adults with evidence of elevated WMH would be most likely to exhibit failures of dynamic allocation of attention. In contrast, we hypothesized that amyloid burden would be unrelated to failures of dynamic allocation of attention. Although amyloid retention is present in the prefrontal cortex, this latter hypothesis arose from our theoretical orientation that multiple pathologies occur during the aging process and have consequences preferential to certain systems (Buckner 2004; Hedden and Gabrieli 2004), while acknowledging the possibility for disruption of more remote systems to occur through multisystem interactions.

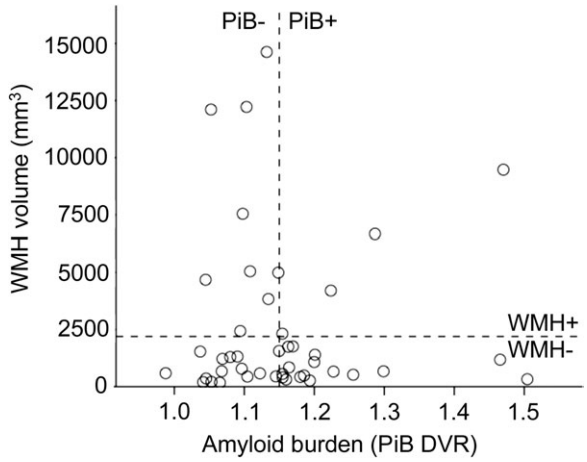

Figure 5. Relationship of white matter disruption and amyloid deposition. WMH volume and amyloid burden (PiB DVR) were measured in individual participants and used to classify individuals into high (WMH+) and low (WHM−) WMH groups and high (PiB+) and low (PiB−) amyloid groups. While many individuals had one or the other of these pathologies, only 4 individuals were classified as being high on both measures, suggesting that these pathologies have distinct etiologies. There was no correlation between the 2 measures of pathology, $r = 0.02$, $P = 0.88$.

Previous associations between amyloid and longitudinal memory declines (Villemagne et al. 2008), hippocampal atrophy (Mormino et al. 2009), and disruption of activity in the default network (Sperling et al. 2009) and its connectivity with the hippocampus (Hedden et al. 2009; Sheline et al. 2010), all suggested that amyloid may primarily influence memory-related systems, whereas attention-related systems may be relatively spared by amyloid pathology.

Using a multiple regression model, we examined the relationship of white matter and amyloid pathologies to the slope of activation among older adults. Because not all individuals had data for WMH volume ($n = 54$) and amyloid burden ($n = 49$), we excluded participants with missing data pairwise to maximize the available data for each analysis. Listwise exclusion did not significantly alter the beta coefficient or model fit estimates. Slope of activation was entered as the dependent variable, and an initial regression of age and average magnitude of activation was conducted to estimate the effects of these potential confounding variables (Table 2, Model 1). A second model added both WMH volume and WMH group (entered as a dummy variable with WMH– as 0, WMH+ as 1) to investigate the effects of WMH pathology and to account for the possibility that such effects occur primarily among older individuals with very elevated levels of WMH. This model resulted in a significant change in R^2 relative to the first model, and the individual coefficients for both WMH volume and WMH group were significant (Table 2, Model 2). However, both WMH volume and WMH group variables must be entered to observe these significant effects, suggesting that the effect is carried primarily by those with elevated WMH volumes (WMH+). This result is visualized in Figure 6*A*.

A third model added amyloid retention (PiB FLR) and amyloid group (entered as a dummy variable with PiB– as 0, PiB+ as 1) but did not result in a significant change in R^2 and neither amyloid variable had a significant coefficient (Table 2, Model 3). This result is visualized in Figure 6*B*. Note that changing the order of entry so that the amyloid variables were entered before the WMH variables did not significantly alter the

Table 2
Regression analyses: slope of activity as dependent variable

Model/variable	β	β_{std}	P_β	R^2	ΔR^2	P_Δ
Model 1				0.16	—	—
Age	.000	0.026	0.840			
Average magnitude	0.078	0.400	0.003			
Model 2				0.26	0.10	0.05
WMH volume	-1.2^{-5}	−0.468	0.023			
WMH group	0.088	0.471	0.021			
Model 3				0.30	0.04	0.38
PiB FLR	0.117	0.153	0.450			
PiB group	0.011	0.062	0.763			

Note: Results of each model are relative to the previous model. Each subsequent model contains variables in the previous model plus the listed variables. Variables were entered in the listed order. β_{std} = standardized beta coefficient.

results. Because FLR DVR is a relatively nonspecific measurement of amyloid burden, we also assessed alternatives to this third model replacing PiB FLR with partial-volume corrected PiB DVR from individual FreeSurfer-defined regions in the frontal and parietal cortices (see Materials and Methods). No individual region was associated with a significant change in R^2 or with a significant beta coefficient (smallest $P_\beta = 0.08$, $P_{\Delta R}{}^2 = 0.12$), and when all amyloid variables were entered simultaneously, no significant results were found ($P_{\Delta R}{}^2 = 0.32$). These results suggest that amyloid does not have a significant influence on the modulation of activity in these attention-related regions, although it is important to note that these null findings are necessarily limited by the power afforded by our sample size and the sensitivity of our measures.

White Matter Burden Mediates the Association between Modulation of Activity and Performance

Using a similar approach, we examined the relationship of slope of activity to task performance. Based on the above results, we hypothesized that white matter burden would mediate the relationship between modulation of activity and task performance. As a single measure of task performance, we computed the slope of the accuracy measurements across conditions (using the same assumption of equal demand intervals applied during computation of the activity slopes) and entered slope of accuracy as the dependent variable in a series of multiple regression models (Table 3). An initial regression of age and average magnitude of activation was conducted to estimate the effects of these potential confounding variables (Table 3, Model 1). A second model added the slope of activity as an explanatory variable and resulted in a significant change in R^2 relative to the first model (Table 3, Model 2; Supplementary Fig. *E*). To test the potential mediating influence of white matter burden on the relationship between modulation of activity and task performance, we examined a third model that entered WMH volume and WMH group in addition to the variables in the first model (Table 3, Model 3). Although the WMH variables were not significantly related to the slope of accuracy, we retained them in the model to test our hypothesis that white matter burden would partially mediate the relationship between slope of activity and slope of accuracy. We tested a fourth model by adding the slope of activity, which did not result in a significant change in R^2 relative to the third model, indicating that white matter burden partially mediates the relationship between modulation of activity and task performance (Table 3, Model 4). Estimations

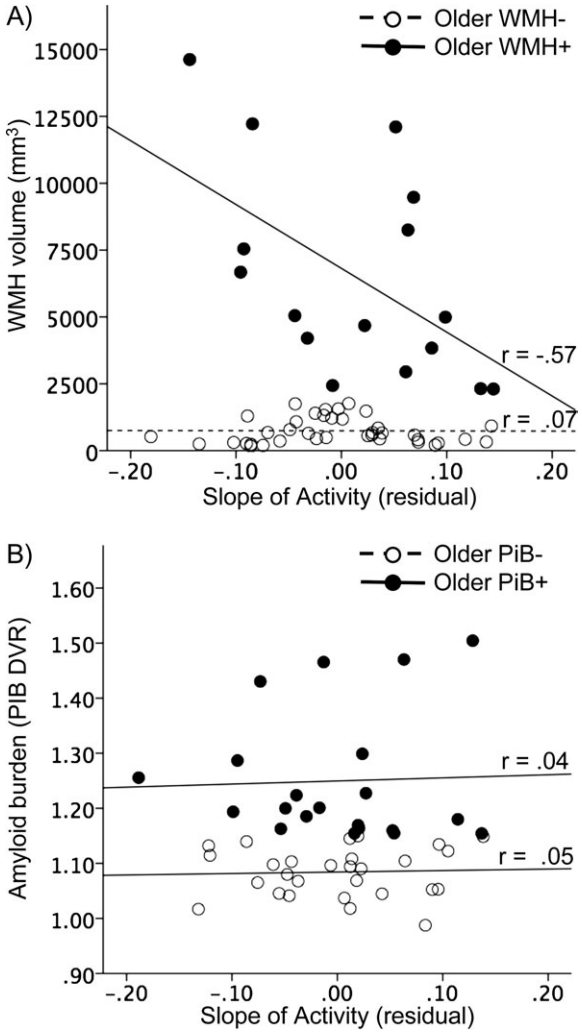

Figure 6. (*A*) WMH volume is associated with failure to modulate activity across conditions. A significant relationship was observed among older individuals with elevated WMH volumes (WMH+), whereas no relationship was observed among those with relatively low WMH volumes (WMH−). These results correspond to those in Table 2, Model 2 and depict the fit lines for the 2 WMH groups separately to visualize the effects in both WMH+ and WMH− groups. The relationship in the total group was not significant, $r = -0.06$, $P = 0.66$. (*B*) Amyloid burden is not associated with activity modulation. Older adults were divided using an a priori threshold into groups with low (PiB−) and high (PiB+) amyloid burden. These results correspond to those in Table 2, Model 3. There was no relationship in either group nor in the total group, $r = 0.03$, $P = 0.86$. Amyloid burden was measured via PiB DVR in the FLR ROI (see Materials and Methods). Dynamic allocation of attention was defined as the residual slope of activity calculated from activity values averaged across prefrontal and parietal ROIs after controlling for age and the average magnitude of activation.

from the change in model fit (ΔR^2) indicated that the WMH variables account for 33% of the variance in the relationship between slope of activity and slope of accuracy. To ensure that this mediating influence was specific to white matter burden, we also tested models that entered amyloid variables (PiB FLR and PiB group) prior to slope of activity (Table 3, Models 5 and 6). Adding slope of activity resulted in a significant change in R^2 (Table 3, Model 6), indicating that amyloid burden did not influence the relationship between modulation of activity and task performance. Estimations from the change in model fit (ΔR^2) indicated that amyloid accounted for 0% of the variance in the relationship between slope of activity and slope of accuracy.

Table 3
Regression analyses: slope of accuracy as dependent variable

Model/variable	β	β_{std}	P_β	R^2	ΔR^2	P_Δ
Model 1				0.11	–	–
Age	−0.002	−0.289	0.022			
Average magnitude	−0.016	−0.162	0.192			
Model 2[a]				0.20	0.09	0.02
Slope of activity	0.153	0.312	0.016			
Model 3[a]				0.16	0.05	0.23
WMH volume	-3^{-6}	−0.232	0.279			
WMH group	0.037	0.360	0.093			
Model 4				0.22	0.06	0.07
Slope of activity	0.131	0.267	0.069			
Model 5[a]				0.17	0.06	0.24
PiB FLR	−0.117	−0.290	0.154			
PiB group	0.007	0.078	0.692			
Model 6				0.29	0.12	0.01
Slope of activity	0.187	0.380	0.011			

Note: Results of each model are relative to the previous model unless otherwise noted. Each subsequent model contains variables in the previous model plus the listed variables. Variables were entered in the listed order. β_{std} = standardized beta coefficient.
[a]Contains all variables in Model 1 plus listed variables, ΔR^2 is relative to Model 1.

Amyloid Burden, But Not WMH Volume, Is Associated with Atypical Activity in the Default Network

In an effort to investigate whether amyloid deposition was related to alterations in default network function within the context of an attentional control task, we examined activity in primary regions of the default network (Shulman et al. 1997; Raichle et al. 2001; Buckner et al. 2008) across conditions. Prior work has demonstrated that amyloid burden is associated with altered activity patterns in the default network during memory encoding tasks (Sperling et al. 2009; Vannini et al. 2011), disruption of resting functional connectivity within this network (Hedden et al. 2009; Sheline et al. 2010), and subtle differences in cortical thickness (Dickerson et al. 2009; Becker et al. 2010). We therefore examined activity in the default network, with the expectation that amyloid might be related to disruption of this activity, whereas WMHs would not be so related. We focused on the magnitude of activity as our primary measure because prior studies have shown an influence of amyloid on magnitude of default activity (Sperling et al. 2009; Vannini et al. 2011).

Defining the network from previous studies (Hedden et al. 2009; Van Dijk et al. 2010), a priori ROIs (Supplementary Fig. *A*) were examined for differences related to amyloid and, separately, WMHs. Activity between regions was highly related (Cronbach's alpha = 0.90), allowing the computation of an aggregate ROI response (mean of all ROIs). Activity (beta values from the GLM) relative to baseline (fixation) was computed for each condition (neutral nonshift, neutral shift, incongruent nonshift, and incongruent shift) in the global–local task for the aggregate ROI and subjected to a PiB group (2) × WMH group (2) × Condition (4) ANOVA. This aggregate ROI exhibited a main effect of PiB group, with greater activity in PiB+ than in PiB– individuals, $F_{1,40} = 4.84$, $P < 0.05$ (Fig. 7A), indicating task-related impairment of activity in those with high amyloid burden. The main effect of WMH group was not significant, $F_{1,40} = 0.64$, $P = 0.43$ (Fig. 7B). There was a main effect of condition, $F_{3,120} = 3.47$, $P < 0.05$, but no other effects were significant. These results are unchanged if age is entered as a covariate in the model. The slope of activity in the default network across conditions (computed in the same manner as in the above analyses) did not differ between the PiB+ ($M = 0.03$,

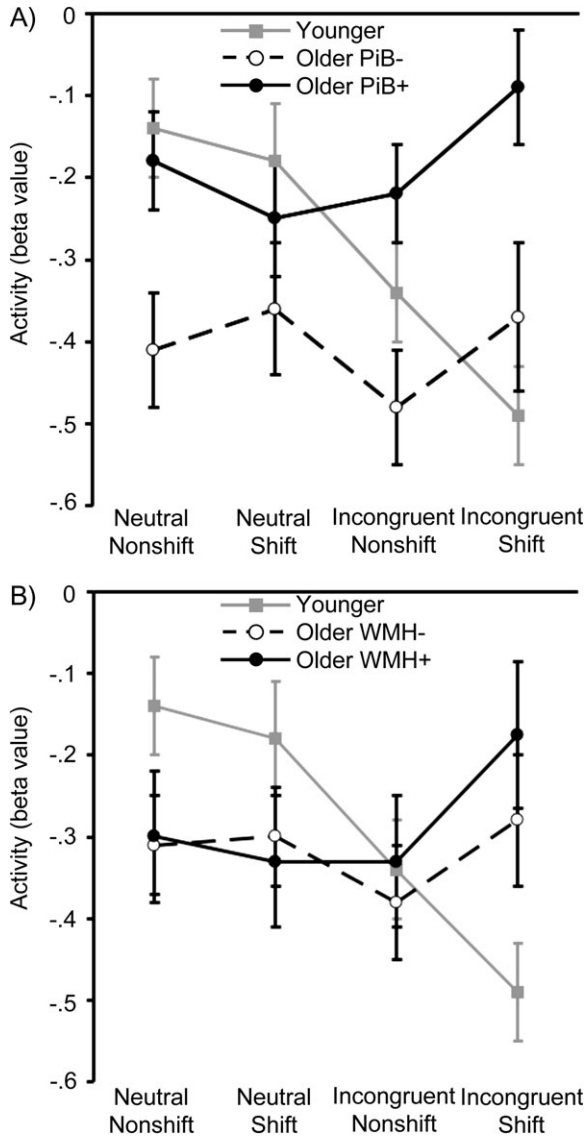

Figure 7. (*A*) Activity in each condition for younger adults and for PiB− and PiB+ older adults averaged across 6 ROIs defining the default mode network. Younger adults exhibited a decrease across conditions, whereas older adults showed no significant change in activity across conditions. PiB+ older adults exhibited less suppression of default mode network activity relative to PiB− older adults. (*B*) Activity in each condition for younger adults and for WMH− and WMH+ older adults averaged across 6 ROIs defining the default mode network. No significant differences were observed between WMH− and WMH+ older adults.

SD = 0.06) and PiB– groups (M = –0.02, SD = 0.12), t_{47} = 1.75, P = 0.09, although the older adults in general (M = –0.01, SD = 0.10) had significantly flatter slopes than did the younger adults (M = –0.12, SD = 0.12), t_{111} = 5.54, P < 0.001 (Fig. 7). This age-related disruption of default activity replicates previous findings (Lustig et al. 2003). We note that the study was not designed to examine default network activity, that these tests are post hoc, and that the study may be underpowered to detect interactions between the PiB and WMH groups because few individuals are in the PiB+/WMH+ group. Therefore, the link between amyloid and default activity in the context of an attentional control task should be interpreted cautiously and verified with replication in other task contexts.

Discussion

We provide evidence that a subset of older adults do not modulate BOLD-measured activity within an attentional control network in response to changing task demands, which we interpret as a failure of dynamic allocation of attention. Failure to modulate activity was associated with increased white matter burden but not with increased amyloid burden. Those older adults who failed to modulate activity displayed poor performance both on the measured MRI task and on an independent composite of executive function. Furthermore, performance decrements observed in older individuals failing to modulate activity did not appear to relate to the absolute magnitude of activity. Older adults as a group exhibited increased magnitudes of BOLD response relative to younger controls, consistent with several prior studies (e.g., Reuter-Lorenz et al. 2000; Cabeza et al. 2002). However, controlling for average magnitude of activity did not affect the relationship between modulation of activity and performance. These results suggest that patterns of reduced activity modulation in response to changing task demands may be a consequence of age-related dysfunction related to neuropathology and behavior.

Some Older Adults Fail to Modulate Activity with Changing Task Demands

As task demands are augmented to include attentional shifting and inhibition, increased activity is typically observed in a network of prefrontal and parietal regions associated with attentional control (e.g., Schneider-Garces et al. 2009; Hedden and Gabrieli 2010). We observed that a subset of older adults failed to display such modulation in response to changes in task demands. The task did not provide any explicit indication that task difficulty was changing so that participants had to track the stimulus history in order to dynamically adjust the level of attentional control exerted. An age-related failure to modulate activity in response to the changes in task demand may therefore indicate an inability to dynamically allocate attentional control in response to changes or an indication that the individual's attentional control is maximally invoked even in the least demanding condition.

To the extent that the best-performing older adults were also those who continued to exhibit increased magnitudes of activity relative to the young across all levels of task demand, the current data are consistent with models that propose increased activity among older adults is compensatory in nature (Cabeza 2002; Reuter-Lorenz and Cappell 2008; Cappell et al. 2010). However, the results suggest a more nuanced explanation. Older adults with nonmodulating activity profiles also displayed increased activity compared with the young in the intermediate conditions accompanied by severely reduced performance. Furthermore, controlling for magnitude of activity did not significantly alter the relationship between modulation of activity and performance. These results suggest that increased magnitude of activity in a given condition (either within group or between groups) is not always a marker of a productive compensatory response. Failure to modulate activity in response to changing task demands may be indicative of dysfunction, even when associated with a pattern of high activity across conditions. It remains possible that age-related differences in vascular reactivity (D'Esposito et al. 2003; Kannurpatti et al. 2010) may account for observed age differences in magnitude of activity, but such accounts do

not explain the observed patterns involving modulation of activity across task conditions.

Amyloid and White Matter Burden Represent Distinct Pathologies in Clinically Normal Older Adults

We measured WMH volume in FLAIR images as a marker of white matter burden (Boone et al. 1992; DeCarli et al. 1995, 2005; De Groot et al. 2000, 2002; Tullberg et al. 2004) and amyloid retention as a pathological marker consistent with preclinical AD (Klunk et al. 2004). We observed no correlation between WMHs and amyloid deposition. Although many older adults exhibited elevated levels for only one of these pathologies, only 4 individuals (9%) in our sample displayed both. Although these results are suggestive of independent etiologies for white matter and amyloid pathologies in clinically normal adults, these data could result from our highly selective screening criteria especially if cooccurring pathologies increase the likelihood of an individual exhibiting clinical symptoms of dementia (DeCarli et al. 1996; Wu et al. 2002; Burns et al. 2005; Head et al. 2005). White matter pathology often accompanies amyloid plaques in advanced AD (Brun and Englund 1986), cerebral amyloid angiopathy provides a link between amyloidosis and vascular infarcts that may result in elevated WMH burden (Johnson et al. 2007; Dierksen et al. 2010), and in vitro data indicate that oligomeric amyloid beta inhibits myelin sheet formation (Horiuchi et al. 2010). Given such results, we cannot rule out the possibility that a relation between these pathologies becomes evident at later stages of disease progression.

Modulation of Activity in Attentional Control Systems Is Associated with Elevated WMHs But Not Amyloid Burden

We observed no significant relationship between amyloid burden and failure to modulate activity. In contrast, we hypothesized that elevated levels of WMHs would be associated with failure to modulate activity in prefrontal–parietal attentional control systems (Tullberg et al. 2004; Nordahl et al. 2006; Venkatraman et al. 2010). Consistent with this prediction, we observed a relationship between elevated WMH volume and failures to modulate activity in attentional control systems, although this relationship was present only among older adults with high levels of WMHs. This relationship should be interpreted cautiously, as some older adults with low levels of WMHs also displayed failures to modulate activity. Hence, it appears that elevated levels of WMHs may be one marker of neural pathology associated with failures of dynamic allocation of attention but do not occur in all individuals with such failures. One possibility is that there are multiple causes of such failures, including those related to synaptic dysfunction and neurotransmitter depletion (e.g., dopamine), as suggested by previous associations with executive function during aging (Erixon-Lindroth et al. 2005; Nagel et al. 2008).

Poor Executive Performance Accompanies Failures to Modulate Activity

Older adults who failed to modulate activity in response to changing task demands performed more poorly on the measured MRI task and on independent composite measures of executive function and speed of processing. This failure to modulate activity may represent an inability of some older adults to flexibly allocate attention to optimize performance or to dynamically track changes in the task structure, which likely detracts from performance to a greater extent as task demands increase. Although modulating older adults performed more poorly than younger adults, modulation of activity among the older adults was associated with improved performance. This relationship was preserved when controlling for the average magnitude of activity, again suggesting that modulation rather than magnitude is an indicator of neural integrity.

Impaired Default Network Activity Is Associated with Amyloid Burden But Not WMHs

Relative to those with low amyloid burden, older adults with substantial amyloid burden showed atypical activity in regions associated with the default network that typically exhibit task-related reductions of activity (Shulman et al. 1997; Mazoyer et al. 2001; for review, see Buckner et al. 2008 and Raichle et al. 2001). In contrast, there were no differences between those with low and high WMH volumes. Together with the finding that WMH volume, but not amyloid, was related to the slope of activity in an attentional control network, these results tentatively suggest a dissociation between these 2 neuropathologies, with white matter pathology disproportionately affecting modulation of an attentional control network and amyloid pathology disproportionately affecting default network activity. Amyloid may preferentially target regions within the default network because of their activity or metabolic properties, in particular the posterior cingulate extending into the precuneus (Buckner et al. 2005, 2009; Vlassenko et al. 2010). Although these results support previous links between amyloid burden and disruption of the default network (Hedden et al. 2009; Sperling et al. 2009; Sheline et al. 2010; Vannini et al. 2011), our study has several limitations that preclude a strong interpretation on this point. Specifically, our study was not designed to target memory processes, and we did not find a significant association between amyloid and memory performance. Further, our ability to examine interactions between amyloid and WMHs was limited by the low number of participants with evidence of high levels of both pathologies. Nonetheless, we discuss these preliminary observations that suggest a dissociation to motivate future explorations.

Conclusion

In summary, a subset of older adults failed to modulate activity in response to changing task demands, a phenomenon we hypothesize to reflect an inability to dynamically allocate attention. This lack of modulation was associated with poorer executive performance and increased WMH volumes among those older adults exhibiting extensive white matter abnormalities but was not related to elevated amyloid burden. Conversely, amyloid burden, but not white matter abnormalities, was associated with evidence of impaired default network activity. These results, in addition to the rarity of co-occurrence between amyloid and white matter pathology among our sample of clinically normal adults, suggest that age-related cognitive failures may arise from multiple distinct pathologies. The observed age differences in failures of attentional allocation were not accounted for by the average magnitude of activity, which was higher among older than younger adults. Age-related failures of dynamic allocation of attention may be an early consequence of disrupted neural integrity within prefrontal–parietal networks.

Supplementary Material

Supplementary material can be found at: http://www.cercor.oxfordjournals.org/

Funding

National Institute on Aging (grants R01 AG021910, R01 AG034556, R01 AG037497, P01 AG036694, and R01 AG027435-S1); Howard Hughes Medical Institute; Alzheimer's Association. K. R. A. V. D. was supported by the Netherlands Organization for Scientific Research.

Notes

We thank Angel Mehta, Renee Poulin, Betsy Hemphill, Jeremy Carmasin, and Meghan Frey for assistance during data collection and Tanveer Talukdar and Itamar Kahn for technical advice. This research was carried out in part at the Athinoula A. Martinos Center for Biomedical Imaging at the Massachusetts General Hospital, using resources provided by the Center for Functional Neuroimaging Technologies, P41RR14075, a P41 Regional Resource supported by the Biomedical Technology Program of the National Center for Research Resources (NCRR), National Institutes of Health. This work also involved the use of instrumentation supported by the NCRR Shared Instrumentation Grant Program and/or High-End Instrumentation Grant Program; specifically, grant numbers 1S10RR023401, 1S10RR019307, and 1S10RR023043. The MGH Molecular Imaging PET Core provided assistance with amyloid imaging. Alex Becker, Aaron Schultz, Bill Klunk, and Chet Mathis provided assistance with PiB. Dorene Rentz and the Massachusetts Alzheimer's Disease Research Center provided assistance with clinical and neuropsychological characterization of the participants. Minjie Wu kindly provided software for labeling WMHs. Research participants were recruited with the assistance of resources provided by the Harvard Cooperative Program on Aging (supported by the Hebrew SeniorLife Institute for Aging Research and grants from the National Institute on Aging 5 P01 AG04390 and the Massachusetts Alzheimer's Disease Research Center Subgrant 2 P50 AG05134), the Research Study Volunteer Program for Health at Massachusetts General Hospital and Brigham and Women's Hospital, and the Commonwealth of Massachusetts Executive Office of Elder Affairs. *Conflict of Interest*: K. A. J. has served as a paid consultant to GE Healthcare, Ltd., which holds a license agreement with the University of Pittsburgh based on the PiB technology described in this article. GE Healthcare provided no grant support for this study and had no role in the design or interpretation of results or preparation of this article.

References

Aizenstein HJ, Nebes RD, Saxton JA, Price JC, Mathis CA, Tsopelas ND, Ziolko SK, James JA, Snitz BE, Houck PR, et al. 2008. Frequent amyloid deposition without significant cognitive impairment among the elderly. Arch Neurol. 65:1509–1517.

Badre D, Wagner AD. 2004. Selection, integration, and conflict monitoring: assessing the nature and generality of prefrontal cognitive control mechanisms. Neuron. 41:473–487.

Becker JA, Hedden T, Carmasin J, Maye J, Rentz DM, Putcha D, Fischl B, Greve D, Marshall G, Salloway S, et al. 2010. Amyloid-β associated cortical thinning in clinically normal elderly. Ann Neurol. doi:10.1002/ana.22333.

Boone KB, Miller BL, Lesser IM, Mehringer CM, Hill-Gutierrez E, Goldberg MA, Berman NG. 1992. Neuropsychological correlates of white-matter lesions in healthy elderly subjects: a threshold effect. Arch Neurol. 49:549–554.

Brainard DH. 1997. The Psychophysics Toolbox. Spat Vis. 10:433–436.

Brun A, Englund E. 1986. A white matter disorder in dementia of the Alzheimer type: a pathoanatomical study. Ann Neurol. 19:253–262.

Buckner RL. 2004. Memory and executive function in aging and AD: multiple factors that cause decline and reserve factors that compensate. Neuron. 44:195–208.

Buckner RL, Andrews-Hanna JR, Schacter DL. 2008. The brain's default network: anatomy, function, and relevance to disease. Ann N Y Acad Sci. 1124:1–38.

Buckner RL, Head D, Parker J, Fotenos AF, Marcus D, Morris JC, Snyder AZ. 2004. A unified approach for morphometric and functional data analysis in young, old, and demented adults using automated atlas-based head size normalization: reliability and validation against manual measurement of total intracranial volume. Neuroimage. 23:724–738.

Buckner RL, Sepulcre J, Talukdar T, Krienen FM, Liu H, Hedden T, Andrews-Hanna JR, Sperling RA, Johnson KA. 2009. Cortical hubs revealed by intrinsic functional connectivity: mapping, assessment of stability, and relation to Alzheimer's disease. J Neurosci. 29:1860–1873.

Buckner RL, Snyder AZ, Shannon BJ, LaRossa G, Sachs R, Fotenos AF, Sheline YI, Klunk WE, Mathis CA, Morris JC, et al. 2005. Molecular, structural, and functional characterization of Alzheimer's disease: evidence for a relationship between default activity, amyloid, and memory. J Neurosci. 25:7709–7717.

Burns JM, Church JA, Johnson DK, Xiong C, Marcus D, Fotenos AF, Snyder AZ, Morris JC, Buckner RL. 2005. White matter lesions are prevalent but differentially related with cognition in aging and early Alzheimer disease. Arch Neurol. 62:1870–1876.

Cabeza R. 2002. Hemispheric asymmetry reduction in older adults: the HAROLD model. Psychol Aging. 17:85–100.

Cabeza R, Anderson ND, Locantore JK, McIntosh AR. 2002. Aging gracefully: compensatory brain activity in high-performing older adults. Neuroimage. 17:1394–1402.

Cappell KA, Gmeindl L, Reuter-Lorenz PA. 2010. Age differences in prefontal recruitment during verbal working memory maintenance depend on memory load. Cortex. 46:462–473.

Colcombe SJ, Kramer AF, Erickson KI, Scalf P. 2005. The implications of cortical recruitment and brain morphology for individual differences in inhibitory function in aging humans. Psychol Aging. 20:363–375.

Craik FIM, Byrd M. 1982. Aging and cognitive deficits: the role of attentional resources. In: Craik FIM, Trehub S, editors. Aging and cognitive processes. New York: Plenum. p. 191–211.

DeCarli C, Grady CL, Clark CM, Katz DA, Brady DR, Murphy DG, Haxby JV, Salerno JA, Gillette JA, Gonzalez-Aviles A, et al. 1996. Comparison of positron emission tomography, cognition, and brain volume in Alzheimer's disease with and without severe abnormalities of white matter. J Neurol Neurosurg Psychiatry. 60:158–167.

DeCarli C, Massaro J, Harvey D, Hald J, Tullberg M, Au R, Beiser A, D'Agostino R, Wolf PA. 2005. Measures of brain morphology and infarction in the Framingham heart study: establishing what is normal. Neurobiol Aging. 26:491–510.

DeCarli C, Murphy DG, Tranh M, Grady CL, Haxby JV, Gillette JA, Salerno JA, Gonzales-Aviles A, Horwitz B, Rapoport SI, et al. 1995. The effect of white matter hyperintensity volume on brain structure, cognitive performance, and cerebral metabolism of glucose in 51 healthy adults. Neurology. 45:2077–2084.

De Groot JC, De Leeuw FE, Oudkerk M, Van Gijn J, Hofman A, Jolles J, Breteler MM. 2000. Cerebral white matter lesions and cognitive function: the Rotterdam Scan Study. Ann Neurol. 47:145–151.

De Groot JC, De Leeuw FE, Oudkerk M, Van Gijn J, Hofman A, Jolles J, Breteler MM. 2002. Periventricular cerebral white matter lesions predict rate of cognitive decline. Ann Neurol. 52:335–341.

Desikan RS, Segonne F, Fischl B, Quinn BT, Dickerson BC, Blacker D, Buckner RL, Dale AM, Maguire RP, Hyman BT, et al. 2006. An automated labeling system for subdividing the human cerebral cortex on MRI scans into gyral based regions of interest. Neuroimage. 31:968–980.

D'Esposito M, Deouell LY, Gazzaley A. 2003. Alterations in the BOLD fMRI signal with ageing and disease: a challenge for neuroimaging. Nat Rev Neurosci. 4:863–872.

Dickerson BC, Bakkour A, Salat DH, Feczko E, Pacheco J, Greve DN, Grodstein F, Wright CI, Blacker D, Rosas HD, et al. 2009. The cortical signature of Alzheimer's disease: regionally specific cortical thinning relates to symptom severity in very mild to mild AD dementia and is detectable in asymptomatic amyloid-positive individuals. Cereb Cortex. 19:497–510.

Dierksen GA, Skehan ME, Khan MA, Jeng J, Nandigam RN, Becker JA, Kumar A, Neal KL, Betensky RA, Frosch MP, et al. 2010. Spatial relation between microbleeds and amyloid deposits in amyloid angiopathy. Ann Neurol. 68:545–548.

Duncan J, Owen AM. 2000. Common regions of the human frontal lobe recruited by diverse cognitive demands. Trends Neurosci. 23:475–483.

Duverne S, Motamedinia S, Rugg MD. 2009. The relationship between aging, performance, and the neural correlates of successful memory encoding. Cereb Cortex. 19:733–744.

Erixon-Lindroth N, Farde L, Wahlin TB, Sovago J, Halldin C, Backman L. 2005. The role of the striatal dopamine transporter in cognitive aging. Psychiatry Res. 138:1–12.

Evans AC, Collins DL, Mills SR, Brown ED, Kelly RL, Peters TM. 1993. 3D statistical neuroanatomical models from 305 MRI volumes. Nuclear Science Symposium and Medical Imaging Conference: IEEE Conference Record. October. 31, 1993, San Francisco, CA (IEEE) New York, NY. 3: p. 1813–1817.

Fagan AM, Mintun MA, Mach RH, Lee SY, Dence CS, Shah AR, LaRossa GN, Spinner ML, Klunk WE, Mathis CA, et al. 2006. Inverse relation between in vivo amyloid imaging load and cerebrospinal fluid Abeta42 in humans. Ann Neurol. 59:512–519.

Folstein MF, Folstein SE, McHugh PR. 1975. Mini-mental state: a practical method for grading the cognitive state of patients for the clinician. J Psychiatr Res. 12:189–198.

Gazzaley A, Cooney JW, Rissman J, D'Esposito M. 2005. Top-down suppression deficit underlies working memory impairment in normal aging. Nat Neurosci. 8:1298–1300.

Gomperts SN, Rentz DM, Moran E, Becker JA, Locascio JJ, Klunk WE, Mathis CA, Elmaleh DR, Shoup T, Fischman AJ, et al. 2008. Imaging amyloid deposition in Lewy body diseases. Neurology. 71:903–910.

Grady CL. 2002. Age-related differences in face processing: a meta-analysis of three functional neuroimaging experiments. Can J Exp Psychol. 56:208–220.

Grady CL, McIntosh AR, Bookstein F, Horwitz B, Rapoport SI, Haxby JV. 1998. Age-related changes in regional cerebral blood flow during working memory for faces. Neuroimage. 8:409–425.

Grober E, Sliwinski M. 1991. Development and validation of a model for estimating premorbid verbal intelligence in the elderly. J Clin Exp Neuropsychol. 13:933–949.

Gunning-Dixon FM, Raz N. 2000. The cognitive correlates of white matter abnormalities in normal aging: a quantitative review. Neuropsychology. 14:224–232.

Gutchess AH, Welsh RC, Hedden T, Bangert A, Minear M, Liu LL, Park DC. 2005. Aging and the neural correlates of successful picture encoding: frontal activations compensate for decreased medial-temporal activity. J Cogn Neurosci. 17:84–96.

Head D, Snyder AZ, Girton Le, Morris JC, Buckner RL. 2005. Frontal-hippocampal double dissociation between normal aging and Alzheimer's disease. Cereb Cortex. 15:732–739.

Hedden T, Gabrieli JD. 2004. Insights into the ageing mind: a view from cognitive neuroscience. Nat Rev Neurosci. 5:87–96.

Hedden T, Gabrieli JD. 2010. Shared and selective neural correlates of inhibition, facilitation, and shifting processes during executive control. Neuroimage. 51:421–431.

Hedden T, Van Dijk KR, Becker JA, Mehta A, Sperling RA, Johnson KA, Buckner RL. 2009. Disruption of functional connectivity in clinically normal older adults harboring amyloid burden. J Neurosci. 29: 12686–12694.

Hollingshead AB. 1957. Two factor index of social position. Mimeo. New Haven (CT): Yale University.

Holtzer R, Rakitin BC, Steffener J, Flynn J, Kumar A, Stern Y. 2009. Age effects on load-dependent brain activations in working memory for novel material. Brain Res. 1249:148–161.

Horiuchi M, Maezawa I, Itoh A, Wakayama K, Jin LW, Itoh T, DeCarli C. 2010. Amyloid beta1-42 oligomer inhibits myelin sheet formation in vitro. Neurobiol Aging. doi:10.1016/j.neurobiolaging.2010.05.007.

Jenkinson M, Bannister P, Brady M, Smith S. 2002. Improved optimization for the robust and accurate linear registration and motion correction of brain images. Neuroimage. 17:825–841.

Jenkinson M, Smith S. 2001. A global optimisation method for robust affine registration of brain images. Med Image Anal. 5:143–156.

Johnson KA, Gregas M, Becker JA, Kinnecom C, Salat DH, Moran EK, Smith EE, Rosand J, Rentz DM, Klunk WE, et al. 2007. Imaging of amyloid burden and distribution in cerebral amyloid angiopathy. Ann Neurol. 62:229–234.

Kannurpatti SS, Motes MA, Rypma B, Biswal BB. 2010. Neural and vascular variability and the fMRI-BOLD response in normal aging. Magn Reson Imaging. 28:466–476.

Kemper S, Schmalzried R, Herman R, Leedahl S, Mohankumar D. 2009. The effects of aging and dual task demands on language production. Neuropsychol Dev Cogn B Aging Neuropsychol Cogn. 16:241–259.

Kennedy KM, Raz N. 2009. Aging white matter and cognition: differential effects of regional variations in diffusion properties on memory, executive functions, and speed. Neuropsychologia. 47:916–927.

Klunk WE, Engler H, Nordberg A, Wang Y, Blomqvist G, Holt DP, Bergström M, Savitcheva I, Huang GF, Estrada S, et al. 2004. Imaging brain amyloid in Alzheimer's disease with Pittsburgh Compound-B. Ann Neurol. 55:306–319.

Klunk WE, Wang Y, Huang GF, Debnath ML, Holt DP, Mathis CA. 2001. Uncharged thioflavin-T derivatives bind to amyloid-beta protein with high affinity and readily enter the brain. Life Sci. 69:1471–1484.

Kwong KK, Belliveau JW, Chesler DA, Goldberg IE, Weisskoff RM, Poncelet BP, Kennedy DN, Hoppel BE, Cohen MS, Turner R, et al. 1992. Dynamic magnetic resonance imaging of human brain activity during primary sensory stimulation. Proc Natl Acad Sci U S A. 89:5675–5679.

Langenecker SA, Nielson KA. 2003. Frontal recruitment during response inhibition in older adults replicated with fMRI. Neuroimage. 20:1384–1392.

Logan J, Fowler JS, Volkow ND, Wolf AP, Dewey SL, Schlyer DJ, MacGregor RR, Hitzemann R, Bendriem B, Gatley SJ, et al. 1990. Graphical analysis of reversible radioligand binding from time-activity measurements applied to [*N*-^{11}C-methyl]-(–)-cocaine PET studies in human subjects. J Cereb Blood Flow Metab. 10:740–747.

Logan JM, Sanders AL, Snyder AZ, Morris JC, Buckner RL. 2002. Under-recruitment and nonselective recruitment: dissociable neural mechanisms associated with aging. Neuron. 33:827–840.

Lopresti BJ, Klunk WE, Mathis CA, Hoge JA, Ziolko SK, Lu X, Meltzer CC, Schimmel K, Tsopelas ND, DeKosky ST, et al. 2005. Simplified quantification of Pittsburgh Compound B amyloid imaging PET studies: a comparative analysis. J Nucl Med. 46:1959–1972.

Lustig C, Shah P, Seidler R, Reuter-Lorenz PA. 2009. Aging, training, and the brain: a review and future directions. Neuropsychol Rev. 19:504–522.

Lustig C, Snyder AZ, Bhakta M, O'Brien KC, McAvoy M, Raichle ME, Morris JC, Buckner RL. 2003. Functional deactivations: change with age and dementia of the Alzheimer type. Proc Natl Acad Sci U S A. 100:14504–14509.

Mathis CA, Bacskai BJ, Kajdasz ST, McLellan ME, Frosch MP, Hyman BT, Holt DP, Wang Y, Huang GF, Debnath ML, et al. 2002. A lipophilic thioflavin-T derivative for positron emission tomography (PET) imaging of amyloid in brain. Bioorg Med Chem Lett. 12:295–298.

Mattay VS, Fera F, Tessitore A, Hariri AR, Berman KF, Das S, Meyer-Lindenberg A, Goldberg TE, Callicott JH, Weinberger DR. 2006. Neurophysiological correlates of age-related changes in working memory capacity. Neurosci Lett. 392:32–37.

Mazoyer B, Zago L, Mellet E, Bricogne S, Etard O, Houde O, Crivello F, Joliot M, Petit L, Tzourio-Mazoyer N. 2001. Cortical networks for working memory and executive functions sustain the conscious resting state in man. Brain Res Bull. 54:287–298.

Miller EK, Cohen JD. 2001. An integrative theory of prefrontal cortex function. Annu Rev Neurosci. 24:167–202.

Mormino EC, Kluth JT, Madison CM, Rabinovici GD, Baker SL, Miller BL, Koeppe RA, Mathis CA, Weiner MW, Jagust WJ. Alzheimer's Disease Neuroimaging Initiative. 2009. Episodic memory loss is related to hippocampal-mediated beta-amyloid deposition in elderly subjects. Brain. 132:1310–1323.

Morris JC. 1993. The Clinical Dementia Rating. CDR: current version and scoring rules. Neurology. 43:2412–2414.

Nagel IE, Chicherio C, Li SC, von Oertzen T, Sander T, Villringer A, Heekeren HR, Backman L, Lindenberger U. 2008. Human aging

magnifies genetic effects on executive functioning and working memory. Front Hum Neurosci. 2:1.
Nagel IE, Preuschhof C, Li SC, Nyberg L, Backman L, Lindenberger U, Heekeren HR. 2009. Performance level modulates adult age differences in brain activation during spatial working memory. Proc Natl Acad Sci U S A. 106:22552–22557.
Navon D. 1977. Forest before trees: the precedence of global features in visual perception. Cognit Psychol. 9:353–383.
Nielson KA, Langenecker SA, Garavan H. 2002. Differences in the functional neuroanatomy of inhibitory control across the adult life span. Psychol Aging. 17:56–71.
Nordahl CW, Ranganath C, Yonelinas AP, DeCarli C, Fletcher E, Jagust WJ. 2006. White matter changes compromise prefrontal cortex function in healthy elderly individuals. J Cogn Neurosci. 18:418–429.
Ogawa S, Tank DW, Menon R, Ellermann JM, Kim SG, Merkle H, Ugurbil K. 1992. Intrinsic signal changes accompanying sensory stimulation: functional brain mapping with magnetic resonance imaging. Proc Natl Acad Sci U S A. 89:5951–5955.
O'Sullivan M, Jones DK, Summers PE, Morris RG, Williams SC, Markus HS. 2001. Evidence for cortical "disconnection" as a - mechanism of age-related cognitive decline. Neurology. 57:632–638.
Park DC, Lautenschlager G, Hedden T, Davidson NS, Smith AD, Smith PK. 2002. Models of visuospatial and verbal memory across the adult life span. Psychol Aging. 17:299–320.
Park DC, Reuter-Lorenz P. 2009. The adaptive brain: aging and neurocognitive scaffolding. Annu Rev Psychol. 60:173–196.
Pelli DG. 1997. The VideoToolbox software for visual psychophysics: transforming numbers into movies. Spat Vis. 10:437–442.
Persson J, Nyberg L, Lind J, Larsson A, Nilsson LG, Ingvar M, Buckner RL. 2006. Structure-function correlates of cognitive decline in aging. Cereb Cortex. 16:907–915.
Persson J, Sylvester CY, Nelson JK, Welsh KM, Jonides J, Reuter-Lorenz PA. 2004. Selection requirements during verb generation: differential recruitment in older and younger adults. Neuroimage. 23:1382–1390.
Price JC, Klunk WE, Lopresti BJ, Lu X, Hoge JA, Ziolko SK, Holt DP, Meltzer CC, DeKosky ST, Mathis CA. 2005. Kinetic modeling of amyloid binding in humans using PET imaging and Pittsburgh Compound-B. J Cereb Blood Flow Metab. 25:1528–1547.
Raichle ME, MacLeod AM, Snyder AZ, Powers WJ, Gusnard DA, Shulman GL. 2001. A default mode of brain function. Proc Natl Acad Sci U S A. 98:676–682.
Rajah MN, Languay R, Valiquette L. 2010. Age-related changes in prefrontal cortex activity are associated with behavioural deficits in both temporal and spatial context memory retrieval in older adults. Cortex. 46:535–549.
Reitan RM. 1955. The relation of the trail making test to organic brain damage. J Consult Psychol. 19:393–394.
Reuter-Lorenz PA, Cappell KA. 2008. Neurocognitive aging and the compensation hypothesis. Curr Dir Psychol Sci. 17:177–182.
Reuter-Lorenz PA, Jonides J, Smith EE, Hartley A, Miller A, Marshuetz C, Koeppe RA. 2000. Age differences in the frontal lateralization of verbal and spatial working memory revealed by PET. J Cogn Neurosci. 12:174–187.
Rypma B, Berger JS, D'Esposito M. 2002. The influence of working-memory demand and subject performance on prefrontal cortical activity. J Cogn Neurosci. 14:721–731.
Salthouse TA. 1996. The processing-speed theory of adult age differences in cognition. Psychol Rev. 103:403–428.
Schmidt M. 1996. Rey Auditory-Verbal Learning Test. Lutz (FL): Psychological Assessment Resources Inc.
Schneider-Garces NJ, Gordon BA, Brumback-Peltz CR, Shin E, Lee Y, Sutton BP, Maclin EL, Gratton G, Fabiani M. 2009. Span, CRUNCH, and beyond: working memory capacity and the aging brain. J Cogn Neurosci. 22:655–669.
Sheline YI, Raichle ME, Snyder AZ, Morris JC, Head D, Wang S, Mintun MA. 2010. Amyloid plaques disrupt resting state default mode network connectivity in cognitively normal elderly. Biol Psychiatry. 67:584–587.
Shulman GL, Corbetta M, Flez JA, Buckner RL, Miezin FM, Raichle ME, Petersen SE. 1997. Searching for activations that generalize over tasks. Hum Brain Mapp. 5:317–322.
Smith SM. 2002. Fast robust automated brain extraction. Hum Brain Mapp. 17:143–155.
Sperling RA, Laviolette PS, O'Keefe K, O'Brien J, Rentz DM, Pihlajamaki M, Marshall G, Hyman BT, Selkoe DJ, Hedden T, et al. 2009. Amyloid deposition is associated with impaired default network function in older persons without dementia. Neuron. 63:178–188.
Spreen O, Benton AL. 1977. Neurosensory center comprehensive examination for aphasia. NCCEA. Victoria (CA): University of Victoria Neuropsychology Laboratory.
Spreng RN, Wojtowicz M, Grady CL. 2010. Reliable differences in brain activity between young and old adults: a quantitative meta-analysis across multiple cognitive domains. Neurosci Biobehav Rev. 34: 1178–1194.
Tullberg M, Fletcher E, DeCarli C, Mungas D, Reed BR, Harvey DJ, Weiner MW, Chui HC, Jagust WJ. 2004. White matter lesions impair frontal lobe function regardless of their location. Neurology. 63:246–253.
Vallesi A, McIntosh AR, Stuss DT. 2011. Overrecruitment in the aging brain as a function of task demands: evidence for a compensatory view. J Cogn Neurosci. 23:801–815.
Van Dijk KRA, Hedden T, Venkataraman A, Evans KC, Lazar SW, Buckner RL. 2010. Intrinsic functional connectivity as a tool for human connectomics: theory, properties, and optimization. J Neurophysiol. 103:297–321.
Van Essen DC, Drury HA, Dickson J, Harwell J, Hanlon D, Anderson CH. 2001. An integrated software suite for surface-based analyses of cerebral cortex. J Am Med Inform Assoc. 8:443–459.
Vannini P, Hedden T, Becker JA, Sullivan C, Putcha D, Rentz D, Johnson KA, Sperling RA. 2011. Age and amyloid-related alterations in default network habituation to stimulus repetition. Neurobiol Aging. doi:10.1016/j.neurobiolaging.2011.01.003.
Velanova K, Lustig C, Jacoby LL, Buckner RL. 2007. Evidence for frontally mediated controlled processing differences in older adults. Cereb Cortex. 15:1033–1046.
Venkatraman VK, Aizenstein H, Guralnik J, Newman AB, Glynn NW, Taylor C, Studenski S, Launer L, Pahor M, Williamson J, et al. 2010. Executive control function, brain activation and white matter hyperintensities in older adults. Neuroimage. 49:3436–3442.
Verhaeghen P, Cerella J. 2002. Aging, executive control, and attention: a review of meta-analyses. Neurosci Biobehav Rev. 26:848–857.
Villemagne VL, Pike KE, Darby D, Maruff P, Savage G, Ng S, Ackermann U, Cowie TF, Currie J, Chan SG, et al. 2008. Abeta deposits in older non-demented individuals with cognitive decline are indicative of preclinical Alzheimer's disease. Neuropsychologia. 46:1688–1697.
Vlassenko AG, Vaishnavi SN, Couture L, Sacco D, Shannon BJ, Mach RH, Morris JC, Raichle ME, Mintun MA. 2010. Spatial correlation between brain aerobic glycolysis and amyloid-β (Aβ) deposition. Proc Natl Acad Sci U S A. 107:17763–17767.
Wakana S, Jiang H, Nagae-Poetscher LM, van Zijl PC, Mori S. 2004. Fiber tract-based atlas of human white matter anatomy. Radiology. 230:77–87.
Wechsler D. 2002. WAIS-III/WMS-III technical manual: updated. San Antonio (TX): Psychological Corporation.
West RL. 1996. An application of prefrontal cortex function theory to cognitive aging. Psychol Bull. 120:272–292.
Wu CC, Mungas D, Eberling JL, Reed BR, Jagust WJ. 2002. Imaging interactions between Alzheimer's disease and cerebrovascular disease. Ann N Y Acad Sci. 977:403–410.
Wu M, Rosano C, Butters M, Whyte E, Nable M, Crooks R, Meltzer CC, Reynolds CF, Aizenstein HJ. 2006. A fully automated method for quantifying and localizing white matter hyperintensities on MR images. Psychiatry Res. 148:133–142.
Yesavage JA, Brink TL, Rose TL, Lum O, Huang V, Adey MB, Leirer VO. 1983. Development and validation of a geriatric depression rating scale: a preliminary report. J Psychiatr Res. 17:37–49.
Zahr NM, Rohlfing T, Pfefferbaum A, Sullivan EV. 2009. Problem solving, working memory, and motor correlates of association and commissural fiber bundles in normal aging: a quantitative fiber tracking study. Neuroimage. 44:1050–1062.